

ARTICLE

## Impact Behaviour of Hybrid Jute/Epoxy Composites at Different Temperature Conditions

Somasundaram Karthiyaini<sup>1</sup>, Mohan Sasikumar<sup>2,\*</sup>, Abraham Jebamalar<sup>3</sup> and P. A. Prasob<sup>2</sup>

<sup>1</sup>School of Civil Engineering, Vellore Institute of Technology, Chennai, 600127, India

<sup>2</sup>School of Mechanical Engineering, Vellore Institute of Technology, Chennai, 600127, India

<sup>3</sup>Department of Civil Engineering, Velammal Engineering College, Chennai, 600066, India

\*Corresponding Author: Mohan Sasikumar. Email: sasikumar.m@vit.ac.in

Received: 10 May 2024 Accepted: 10 July 2024 Published: 16 December 2024

### ABSTRACT

This manuscript presents the projectile impact behavior of hybrid jute/epoxy composite laminates using an instrumented air gun impact setup with the projectile moving in the vertical direction. An approach based on the stiffness change is used to predict the projectile impact response of hybrid jute epoxy-filled laminates impacted with a stainless-steel projectile. The experimental validation of the parameters like dynamic hardness (Hd) coefficient of restitution (COR), natural frequency, damping factor, and loss factor was used to analyze the impact behavior of jute/epoxy composites strengthened with fillers ZrO<sub>2</sub>, ZnO, and TiO<sub>2</sub>. The free vibration tests of the pre-and post-impacted filled hybrid composites give the natural frequency and damping characteristics at room temperature and subzero temperatures. The results show that the stiffness of the laminates increases with the increase of Hd and COR. The natural frequency of the composite laminates was lower for the laminates subjected to higher velocity impact compared to the laminates subjected to the lower impact velocity. The analysis of the damping factor and loss factor shows that damping was better at subzero temperatures compared to room temperature.

### KEYWORDS

Damping; natural frequency; sub-zero temperature; impact loading; nanocomposite

## 1 Introduction

The thorough thickness strengthening mechanisms of the natural fiber composites help improve the impact resistance, thereby allowing the natural fiber composites to have mechanical properties equaling that of synthetic fiber composites. Even though synthetic fiber composites exhibit better impact resistance, the non-degradable nature of the synthetic composites creates environmental problems. Here the jute/epoxy composites strengthened with the use of ceramic fillers ZnO, ZrO<sub>2</sub>, TiO<sub>2</sub> is subjected to projectile impact with an in-house experimental setup at room temperature and subzero temperature conditions. The high damping capacity of the natural fiber composites filled with nano-fillers makes them highly preferred for structural applications while the difference in the thermal contraction of the matrix, fillers, and fibers induces stresses which amount to highly



unpredictable behavior during impact at subzero temperatures. However, the highly unpredictable impact behavior of the natural fiber composites under subzero temperature is analyzed for the free vibration characteristics of the composite plates before and after the projectile impact. The natural frequency of the specimen can be correlated to the extent of damage while testing the samples below the projectile limit. The first mode of the free vibration is given due importance as the frequency in the first mode can explain the free vibration characteristics in the case of projectile impact. Natural fiber composites are used for structural applications, as inliner of automobile doors and carry cases for ammunition dropped from aircraft at higher altitudes.

Flax and carbon fibers reinforced polymer composites have high potential to be used as sustainable building materials. The damage resistance, impact response, and impact tolerance were investigated using drop hammer impact tests [1]. Natural fibers have gained the interest of researchers due to their low cost, availability, sustainability, and biodegradable properties, and also as reinforcement material in polymer composites. The mechanical and tribological properties of these engineered biocomposites are improved by adding nanoparticles like  $ZrO_2$ ,  $SiO_2$ ,  $CuS$ ,  $ZnO$ ,  $CuO$ , and  $TiO_2$  into polymer matrices [2]. The impact resistance and damage tolerance of fiber-reinforced composite are affected by various factors such as fabric architecture, resin toughness, impactor geometry, stacking sequence, and fiber/matrix hybridization. Fabric architecture and resin toughness are the most important factors in improving the impact resistance and damage tolerance of composites [3].  $ZnO$  was dispersed in polyester laminates, fabricated by hand lay-up technique followed by compression molding. Flexural strength of 3 wt.%  $ZnO$  filled GFRP composite was improved significantly (up to 62.12%) in comparison to the unfilled composite. Hardness, impact strength and thermal stability have also been found to increase gradually with an increase in  $ZnO$  loading [4].

The energy dissipation patterns obtained from the load-deflection curves of BFML (basalt fiber metal laminate) plate, BFRP (basalt fiber-reinforced polymer) panel, and aluminum sheet during impact perforation showed that BFMLs and aluminum alloy had negligible strain rate changes, while BFRP had appreciable strain rate changes. Ignoring the energy absorbed in debonding, it was observed that the energy absorption of the aluminum sheet through pedaling and plastic deformation and is nearly 20%, and nearly 75% of the energy is absorbed by BFMLs during drop weigh impact event [5]. The cone formation at the rear face of the composite plate, matrix cracking, delamination, and friction between laminate and projectile during penetration is taken as the energy-absorbing mechanisms during ballistic impact. The impact event's contact duration depends on the incoming projectile velocity. The correlation of the nose shape and damage area shows that impact with conical shaped projectile leads to minimum damage area and the truncated projectile creates the maximum damage area for the same velocity of impact [6]. The polymer composites exposed to moist cryogenic conditioning experience changes in their mechanical properties. Also, the micro filler addition leads to enhanced mechanical strength even at cryogenic temperatures. The low-velocity impact testing of PMC at cryogenic temperatures shows that the impact resistance decreases at lower temperatures. The residual compressive buckling strength and the elastic modulus have an inverse effect on the impact damage and temperature [7].

The target absorbs the energy lost by the projectile during impact using compression of the region of impact and the surrounding regions of the impact. The deformation on the rear face of the target, failure and deformation of the secondary, and primary yarns friction between the target and the projectile, matrix cracking, and delamination, all contribute to the energy-absorbing part in ballistic impact [8]. The effect of impact damage and temperature on residual compressive buckling strength and elastic modulus were inversely proportional [9]. The parameters of impact velocity, geometry of the projectile, boundary conditions, fabric architecture, material properties of the yarn, and friction effect affect the penetration resistance of a fabric subjected to ballistic impact [10]. The analysis of the

ballistic impact of glass fiber laminates using Abaqus/Explicit software shows that cross-ply laminates have improved ballistic resistance compared to the laminates of different orientations [11].

Reddy et al. [12] revealed that the laminate thickness and energy absorption of E-glass/phenolic composites show a non-linear relationship when impacted at various velocities using 7.62 mm mild steel projectile. The energy absorption of the laminates depends on the interaction time of impact, which indirectly depends on the laminate thickness and velocity. The cross-section analysis of the higher and lower-thickness laminates shows that the damage area increases as the thickness increases. The difference in laminate thickness creates different damage mechanisms upon impact. The existence of delamination threshold load (DTL) is discussed in relation to the impact of energy and laminate stiffness/thickness. Compression-after-impact testing is recommended for finding the residual compressive strength of the damaged specimen [13]. The hybrid composite of jute/glass fiber-reinforced composites exhibits higher impact resistance compared to the jute fiber-reinforced composites. The relationship between the drop height and the identified damaged areas are found to be linear. The impact test analysis shows that the JFRC has higher energy absorption compared to hybrid jute/glass fiber reinforcement [14]. The parameters geometry of the specimen, environmental conditions, material, and the impact event affect the impact resistance and damage mechanics of the fiber-reinforced composites [15].

The total impact energy as a sum of rebounding energy, membrane energy, bending energy, and delamination energy of unidirectional, woven, and multi-axial warp-knit Kevlar fabric composite laminates is evaluated. The wrap-knit composites have better bending properties, and higher impact fracture toughness resulting in reduced delamination and increased bending energy. The woven composites have delamination energy as the dominant energy absorption mode [16]. The energy absorption in delamination, failure, deformation of primary and secondary yarns, and matrix crack is predicted with the help of a mathematical model which can also predict the energy change in the projectile as it perforates the laminates. The addition of clay up to 5% by weight shows an increase in energy absorption, and at the ballistic, there is 70% energy absorption by bending for the clay-filled laminates [17]. The dynamic mechanical analysis (DMA) indicates that impact properties and residual flexural strength are better for hybrid composites as compared to non-hybrid composites. Three-point bending test, along with acoustic emission monitoring shows decreased residual flexural strength and impact strength at elevated temperatures [18]. The E-glass (woven) epoxy laminate exposed to an impact velocity of 4.429 m/s and impact energies of 3 to 15 J exhibited crack initiation and perforation of the laminate and the tests confirm that the elastic nature of the fiber material can be correlated to the dynamic response [19].

The jute/epoxy composite shows a nonlinear behavior while tested for tensile strength. Also, the effect of stacking on energy absorption shows that [45°] 5 configurations absorb maximum energy [20]. The treatment for improving the adhesion of the fillers with the matrix increases the load-bearing capacity, and strength of the composite laminates and decreases the ductility indices [21]. Ballistic impact testing focuses on the ductile-brittle transition of metals and is considered an essential testing method for strength characteristics and energy absorption of structural elements [22]. Impact resistance of the (0/90) woven composite laminates is higher compared to any other lay-up of laminates. The damaged area decreases with increasing velocities above the ballistic limit for the composite's laminates. The energy absorption and ballistic limit increase with the increase in failure strain and dynamic Young's modulus of the laminates [23]. The gas gun experimental setup was used to analyze the impact loading of woven carbon-fibre reinforced poly (ether-ether ketone) (CF/PEEK) composites. The experimental set up also uses a three-dimensional Digital Image Correlation (DIC) system to assess the damage of the woven composite [24].

The preloaded woven glass/polyester composite laminate shows improved impact resistance with the ballistic limit of the composites increasing by 11% compared to the unloaded composite laminates [25]. The improved impact resistance of glass/epoxy composites filled with silicon carbide makes them a suitable choice for dashboards and bumpers in automobiles and also as the casing for hot and cold and storage boxes [26]. The combination of finite element analysis code and the modified Hertz law used to analyze the low-velocity impact behaviour of woven fabric composites shows that the damage resistances of the woven fabric laminates are comparatively better than that of cross-ply laminates. The in-plane damage resistance of the composites is evaluated based on the Tsai-Hill quadratic failure criterion [27].

The damage induced in liquid nitrogen-cooled CFRP composites is identical to that of damage induced at higher impact energies as evident from the down-reaching indentation starting from the impacted face, delamination extension, severe debonding of the fiber and matrix, larger matrix cracking. The impact loads at lower temperature contribute to the initiation and propagation of damage. As the temperature changes from  $-20^{\circ}\text{C}$  to  $-150^{\circ}\text{C}$ , the decrease in the threshold energy in quasi-isotropic laminate is around 50% [28]. The extent of shear deformation as a result of the ballistic impact is dependent on the in-plane shear modulus of the composite plates. The total energy lost by the projectile during ballistic impact is the sum of energy involved in the development of the moving cone on the rear side of the target plate, elastic deformation of the composite, and energy absorbed in the tensile failure [29]. The improved specific energy absorption (9%–67%), lower peak load (5%–45%), higher ductile indices (8%–220%), in the weft and warp directions are shown by the interply hybrid composites in comparison to the interply composites when impact tested at velocities of 2 and 3 m/s [30].

The static punch curve simulation using ring elements is carried out on the penetration of long and short projectiles. The nonlinear behaviour of the thick composite laminates during the penetration is captured using the static punch curve 'structural constitutive model' which is also used for the prediction of ballistic limits and residual velocities for different projectile lengths, target thickness and sizes. The delamination area of the composite specimen expands with the increase of impact velocity until the ballistic limit is reached [31]. The short carbon fiber and Carbon Nanotube (CNT) reinforced polymer matrix including the interphase is modeled as representative volume elements. The finite element analysis of the model predicts the density and the modulus of the material and low velocity impact shows that the stiffness of the material is improved by the addition of CNT and SCF [32]. The carbon fiber/CNT nano-composites of polymer matrix are modeled to predict the mechanical properties using a micromechanical approach. The analysis of the model is carried out using the variational differential quadrature technique. The analysis predicts that the addition of the CF/CNT improves the peak contact forces, and reduces the deformation when subjected to low velocity impact [33]. The micromechanical model of the metal matrix nano-composite of silicon carbide is analyzed with the finite element method to investigate the effect of volume fraction, agglomeration of SiC nanoparticle, the effect of the projectile radius and velocity on the specimen size and boundary conditions [34]. The effect of matrix and reinforcements of the polymer matrix composites is analyzed by correlating the mechanical properties with the dynamic hardness and co-efficient of restitution using a gravity drop system and a tungsten carbide projectile [35].

The addition of  $\text{SiO}_2$  nanoparticles with the epoxy matrix enhanced the energy absorption and contact forces. The energy absorption increased from 18.1 to 24.87 J at cryogenic temperatures for pure epoxy resin while energy absorption was 22.7 J for the filled epoxy composites [36]. The impact resistance of the composite is improved with the addition of 1–2 wt.%  $\text{Al}_2\text{O}_3$  nanoparticles. Then the bending stiffness and contact stiffness of the composite were found to improve with addition of 2 wt.% alumina [37]. The impact resistance of Halloysite nanotubes filled multiscale composites has improved the impact loading resistance by nearly 13% as compared to the pristine composites. Moreover, it can

be seen that the impact resistance of sea water-aged composite joints was reduced by 30% [38]. The addition of Halloysite Nanotubes (HNT) with the epoxy matrix of epoxy/basalt composite improved the impact resistance of multiscale composites by 15% at lower impact energy levels [39]. The threshold load, rebound energy, and contact stiffness of carbon fiber epoxy composites was found to enhance with the addition of 2 wt.%  $\text{CaCO}_3$  in the matrix. The critical threshold forces improved by 16.8%, 13.4%, and 11.3% at 2, 2.5, and 3 m/s velocities of impact respectively. Crack pinning, crack deflection, and nanoparticle debonding was found to be the toughening mechanism of the composite [40].

The composite plates are manufactured by strengthening the plates in the thickness direction with the addition of ceramic fillers. The jute/epoxy-filled nano-composites are exposed to impact energy of 30, 25 and 20 J with the help of an in-house setup. The impact velocity of the projectile is calculated from IR sensors programmed to calculate the time in microseconds for a known displacement journey of the projectile. The variation of stiffness at different velocities of impact at subzero and room temperature conditions is correlated to the coefficient of restitution and dynamic hardness. The damage of the composite is quantified based on the vibration parameters, natural frequency, and damping of the plates before and after impact using the impact hammer test setup. The response of the accelerometer obtained as the result of the impact hammer excitation gives the different modes of vibration of the specimen. The projectile impact behavior of woven jute fiber polymer composites strengthened with ceramic fillers at subzero temperature condition is first of its kind as no other literature is reported elsewhere.

## 2 Materials and Experimental Procedure

### 2.1 Materials and Methods

The Huntsman epoxy LY-556 and hardener HY-951 along with bi-directional woven jute fabric and fillers is used for the production of the composite specimens. The properties of the jute fiber (0/90 orientation, plain weave), zirconium dioxide, titanium dioxide, and zinc oxide nanofillers are given in Table 1. The percentage of micro fillers that can be added to the matrix for composite manufacturing differs from 10% to 50 % while nanofiller addition above ten percent by weight with the matrix will form agglomerates and there will be non-uniform distribution of the fillers resulting in substandard adhesion of the fillers at the matrix filler interface. The high-energy ball milling with a speed of 250 rpm is used to synthesize the nano-fillers  $\text{TiO}_2$ ,  $\text{ZnO}$  and  $\text{ZrO}_2$ . The nano-fillers are then added to the epoxy matrix and hardener by mixing them using a mechanical stirrer. The six-layered laminates manufactured by the hand lay-up method are heat-treated at  $80^\circ\text{C}$  for 2 h for better curing. The volume fraction of the jute fabric used in the hand layup manufacturing of the specimens is 39. The hybrid composite plates are made with an initial size of  $800\text{ mm} \times 800\text{ mm} \times 6.6\text{ mm}$  and then cut to size to have an impact area of  $250\text{ mm} \times 250\text{ mm}$  for projectile impact testing as shown in Fig. 1.

**Table 1:** Materials properties

Constituents	Specification	Properties
Reinforcement	Jute fiber (Woven)	Density = $1.5\text{ g/cm}^3$
Epoxy	LY-556	UTS 82MPa, Density = $1\text{ g/cm}^3$
Hardener	HY 951	UTS 50 MPa, Density = $0.98\text{ g/cm}^3$
Nano Fillers	$\text{TiO}_2$ , $\text{ZnO}$ , $\text{ZrO}_2$	Density = 5.6, 3.9, $5.89\text{ g/cm}^3$ , Diameter 100–120 nm

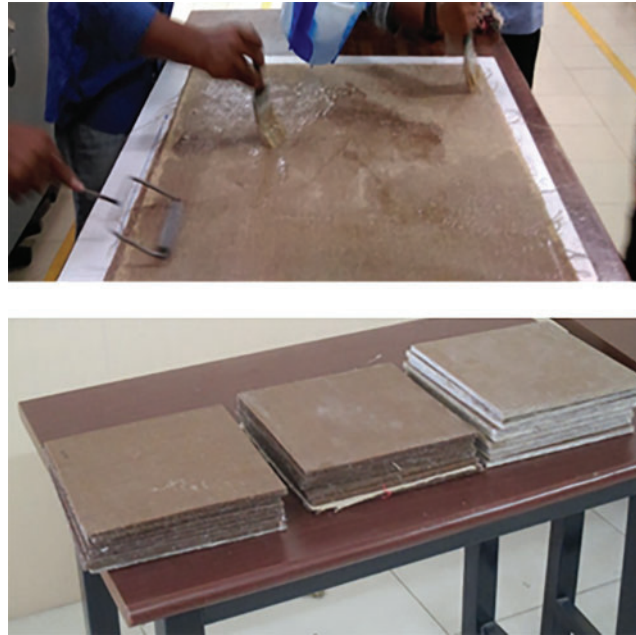


**Figure 1:** Manufacturing filled jute/epoxy composite plates

The static testing is carried out to find the strength characteristics like the tensile, flexural and inter-laminar shear strength at temperature variations of  $-40^{\circ}\text{C}$  and  $27^{\circ}\text{C}$  in the unfilled condition and filled conditions of 2 and 4 wt.% of all three filler combinations of the jute/epoxy composites. The dynamic characteristics like the coefficient of restitution, dynamic hardness, absorbed energy, natural frequency, damping factor, loss factor is also found at temperature conditions of  $-40^{\circ}\text{C}$  and  $27^{\circ}\text{C}$  with unfilled condition and filled conditions of 2 and 4 wt.% of all three filler combinations. The dynamic characteristics of all combinations are tested at three different velocities of 20, 30 and 40 m/s. The damage area of the jute/epoxy composites is also determined based on the unfilled and filled conditions of 2 and 4 wt.% at  $-40^{\circ}\text{C}$  and  $27^{\circ}\text{C}$  under different velocity conditions of projectile impact. The research methodology is summarized in [Fig. 2](#).

## 2.2 Projectile Impact

The projectile impact test was carried out using a newly developed pneumatic test rig prepared with a velocity measurement system attached to the guide tube shown in [Fig. 3](#). The solenoid valve connecting the air storage tank and the guide tube helps in varying the air pressure, thereby allowing the user to have different velocities of impact on the target plate. The initial velocity is imparted to the projectile using the compressed air of the storage tank. The point of impact at the center of the composite plate is made possible with the use of a guide tube, which allows the bullet of 15 mm diameter to pass through without much friction. The velocity of the projectile is calculated by measuring the time taken by the projectile to cover a known distance of 200 mm. The time is calculated with the help of an automated counter system which receives input from two infra-red probes. As soon as the projectile obstructs the infrared rays, the counter system starts to count and as the projectile obstructs the infrared ray focused to a receiver placed 200 mm from the first receiver the counter stops counting and the net time is taken, and the velocity is calculated from the known displacement. In this study, filled polymer composite is tested under three different medium velocity ranging from 20 m/s to 40 m/s at room temperature and subzero temperature of  $-40^{\circ}\text{C}$ . A mild steel impactor of diameter 15 mm and semispherical nose shape and is used as the projectile. The fixture mounted hybrids specimens

250 mm × 250 mm are clamped on all sides to restrict rotational and transitional movements. A cooling chamber and an isolation environment ensure a minimum rate of heating from sub-zero temperatures to ambient conditions. The specimens are exposed to liquid nitrogen so that the specimens attain  $-45^{\circ}\text{C}$  and are finally tested when the temperature of the specimen reaches  $-40^{\circ}\text{C}$ .

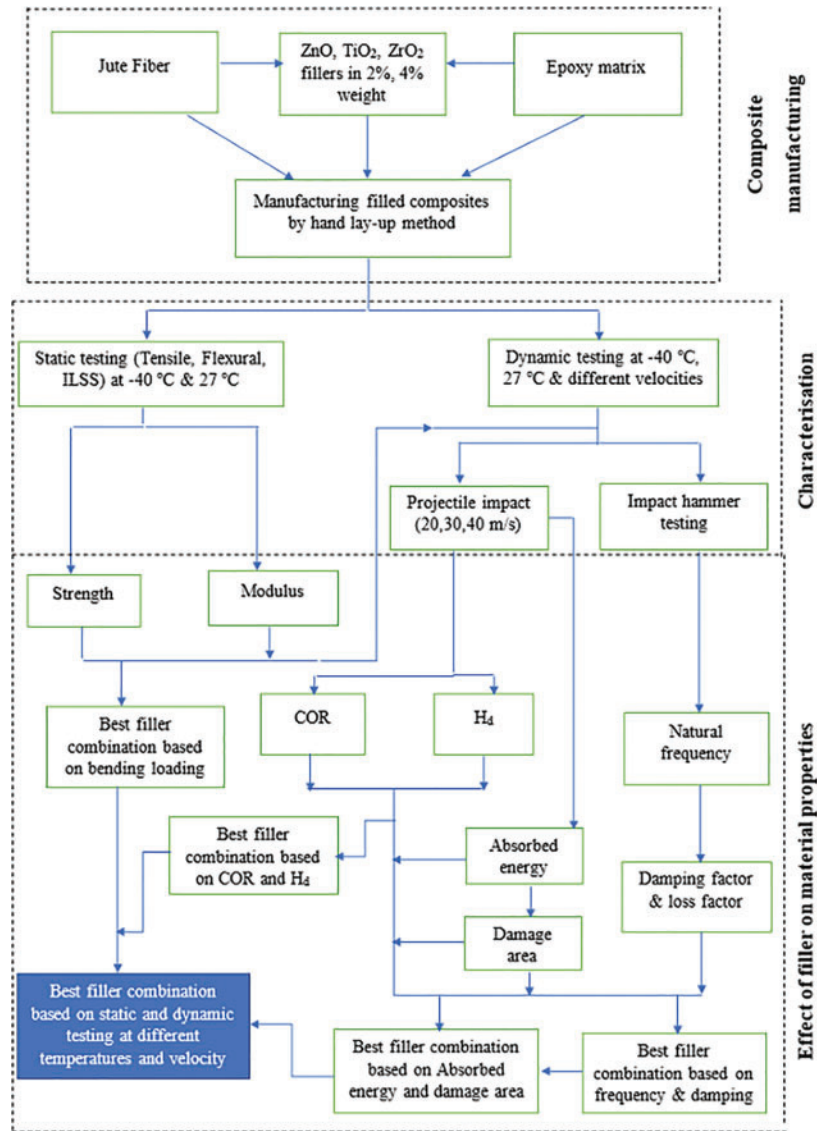
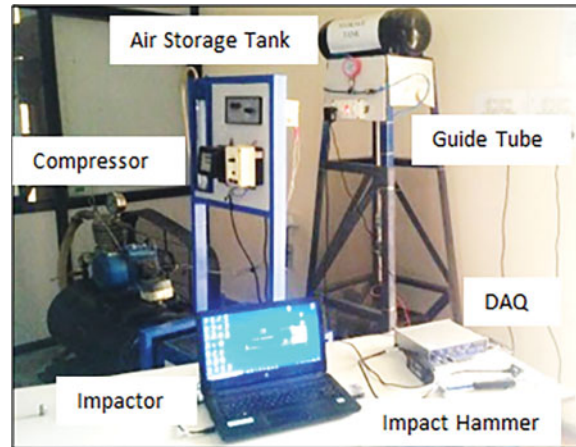


Figure 2: Research methodology

### 2.3 Free Vibration Testing

Vibration testing with impulse using impact hammer and frequency response is effectively utilized for finding the damping factor and natural frequency. The filled laminates are subjected to vibration test before and after impact using the mild steel hemispherical bullet at different velocities. Also, for subzero temperature conditions, the hybrid composite specimens are excited before and after exposure to liquid nitrogen. Finally, the sample is tested with the projectile for different velocities followed by testing the samples using the impact hammer for free vibration behavior. The response of the laminate excited with an impulse hammer is picked up by an accelerometer fixed in a non-damaged area or

along a non-nodal line. The exact location of the accelerometer is 1/4th of the diagonal length from the laminate centre. The impact hammer is used to excite the laminate near the impact area. The FFT is used for computing the frequency response of the response and excitation signals used as inputs to the m + p Analyzer. The peaks of the frequency response curve are the natural frequencies of the hybrid composites. The half-power bandwidth method is used for calculating the damping factor for the jute/epoxy hybrid composite plates, as shown in Fig. 4.



**Figure 3:** Projectile impact experimental setup

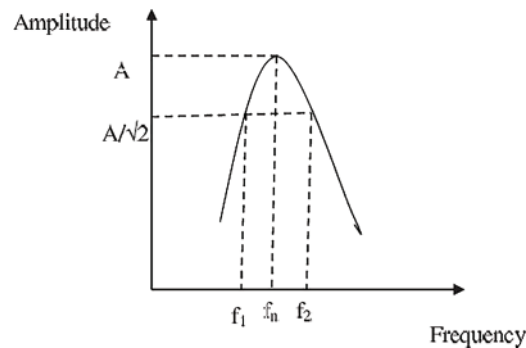


**Figure 4:** Frequency response function for assessing the damping factor

The damping factor  $\xi$ , is given as

$$\xi = (f_2 - f_1)/2f_n \quad (1)$$

where  $f_n$  is the resonance frequency;  $f_2$  and  $f_1$  are the upper frequency and lower frequency.

### 3 Results and Discussion

#### 3.1 Co-Efficient of Restitution and Dynamic Hardness

The coefficient of restitution of the composites specimens is calculated based on the velocity measurements of impact and rebound, whereas the dynamic hardness is calculated from the Eq. (4) [31]. The following assumptions are made while calculating the coefficient of restitution. The time-dependent deformation behaviour of the filled composites is ignored, and the deformation is taken as



time-independent deformation. The resulting deformation is adiabatic as well.

$$COR = \frac{1.9H_d^{5/8}}{E_{eff}^{1/2} \rho_b^{1/8} V^{1/4}} \quad (2)$$

The coefficient of restitution 'COR' is related to the dynamic hardness  $H_d$  as given in Eq. (2).

$$E_{eff} = \frac{E_b E_f}{(1 - V_b^2) E_s + (1 - V_s^2) E_b} \quad (3)$$

The effective modulus of the composite plate target and the mild steel projectile is given in Eq. (3).

$$H_d = 0.36(COR)^{8/5} E_{eff}^{4/5} \rho_b^{1/5} V^{2/5} \quad (4)$$

The dynamic hardness of the filled composite target is given in equation four.

$\rho_b$  = density of the composite target plate;  $V$  = impact velocity and  $E_{eff}$  = effective modulus of the target and projectile [31].

The impact velocity and temperature influences the coefficient of restitution (COR) of the projectile and the target plate, as shown in Fig. 5A–C. The COR and  $H_d$  are highest for the ZrO<sub>2</sub> filled composites, and lowest for the ZnO-filled composites. As the impact velocity increases the COR decreases and as the temperature decreases the COR increases and vice versa. It is evident from the values that modulus has a better correlation with COR and  $H_d$ . The experimental data revealed that the COR and dynamic hardness is higher for the hybrid composites with higher stiffness. i.e., the results clearly show that as the COR and  $H_d$  increases, the stiffness of the composites increases and vice versa. The temperature and impact velocity has a major influence on COR and dynamic hardness. The COR and  $H_d$  are higher at sub-zero temperatures compared to the ambient conditions. Also, it is found that decreasing the velocity and temperature increases the COR and  $H_d$  and vice versa. Also, the COR and  $H_d$  are highest for the ZrO<sub>2</sub> filled composites and the lowest for the ZnO-filled composites.

The hardness of the target subjected to projectile impact may be interpreted as the target polymer composite plate offering a constant pressure of resistance to the indenter numerically equal to the ratio (energy of indenter)/(volume of indentation). This ratio is known as the dynamic hardness number and the ratio has the same dimensions of pressure. The projectile impact is divided into three main parts, the elastic deformation of the target surface which develops mean pressure sufficient to cause deformation when impacted with the projectile until the plastic deformation of the jute epoxy filled composite. The elastic stresses are developed in the jute epoxy hybrid composite target and the projectile followed by the plastic or permanent deformation of the target plate until the projectile comes to rest. The material relaxation due to the release of elastic stresses results in the rebound of the projectile. The event of indentation yields dynamic pressure which can be more than the static pressure required for the plastic flow of the targeted jute epoxy composite plate. The plastic deformation due to impact occurs as long as the pressure applied by the projectile impact is equal to the dynamic pressure and from there on plastic flow continues even if the pressure remains constant.

As the velocity of impact increases the dynamic hardness number decreases as shown in Fig. 6A–C, irrespective of the fillers used in the composite plates. Also, at sub-zero temperatures, the dynamic hardness numbers are higher compared to the ambient conditions with 4 wt.% of filler additions having the highest hardness number. From the filler's perspective, ZnO filled jute/epoxy composites exhibits minimum dynamic hardness as shown in Fig. 6A followed by the TiO<sub>2</sub> filled composites and the maximum hardness are shown by the ZrO<sub>2</sub> filled composites as shown in Fig. 6C. From the definition of the dynamic hardness number, it can be proved that the volume of indentation is lesser in the case of the ZrO<sub>2</sub> filled jute/epoxy composites as the energy of the projectile remains for a particular velocity

of impact. The plastic deformation which follows the elastic deformation once the intender strikes the composite target plate is lesser due to the higher mechanical strength of the  $ZrO_2$  filler. The  $ZrO_2$  filler seems to have better filler dispersion from among the different fillers used and helps in forming better interface for transmitting the load from the projectile impact.

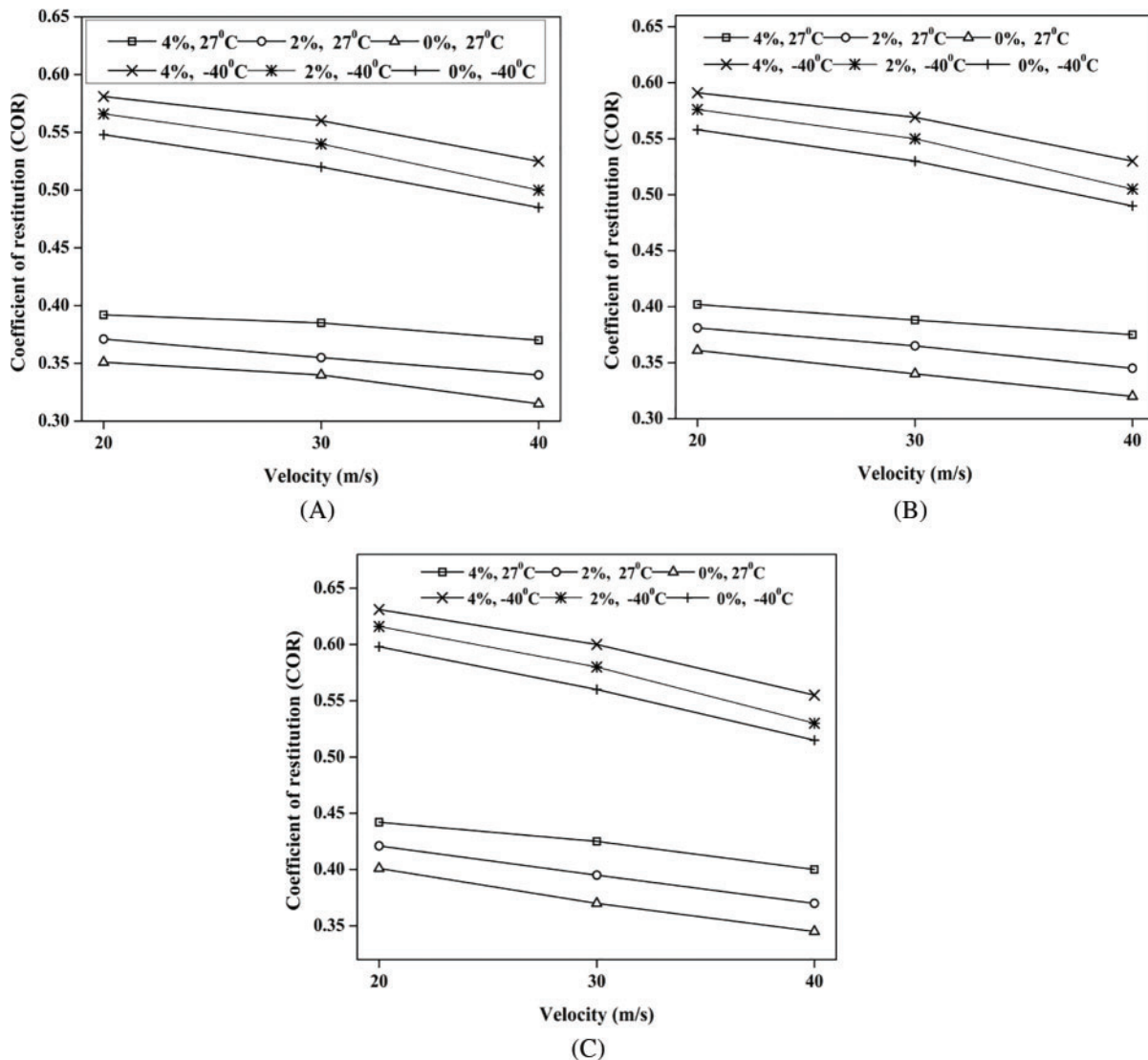


**Figure 5:** (A) Coefficient of restitution of ZnO filled jute/epoxy; (B) Coefficient of restitution of TiO<sub>2</sub> filled jute/epoxy; (C) Coefficient of restitution of ZrO<sub>2</sub> filled jute/epoxy

### 3.2 Absorbed Energy

The impact on the viscoelastic hybrid jute/epoxy composites consists of a compression phase and a rebound phase. The rebound phase starts after the dissipation of all the kinetic energy in the compression phase. The release of the stored elastic energy during impact gives rebound to the projectile and the rebound velocity is a measure of the stored energy. The energy stored during the contact duration is due to the viscoelastic nature and the plastic deformation of the jute/epoxy hybrid composites. The absorbed energy of the filled composites subjected to impact at 20, 30, 40 m/s velocity at room temperature and subzero temperature is given in Fig. 7A–C, respectively. The absorbed energy

increases with the impact velocity irrespective of the temperature. Irrespective of the filler, the absorbed energy increases with the increase in weight percentage of filler added to the hybrid composite.

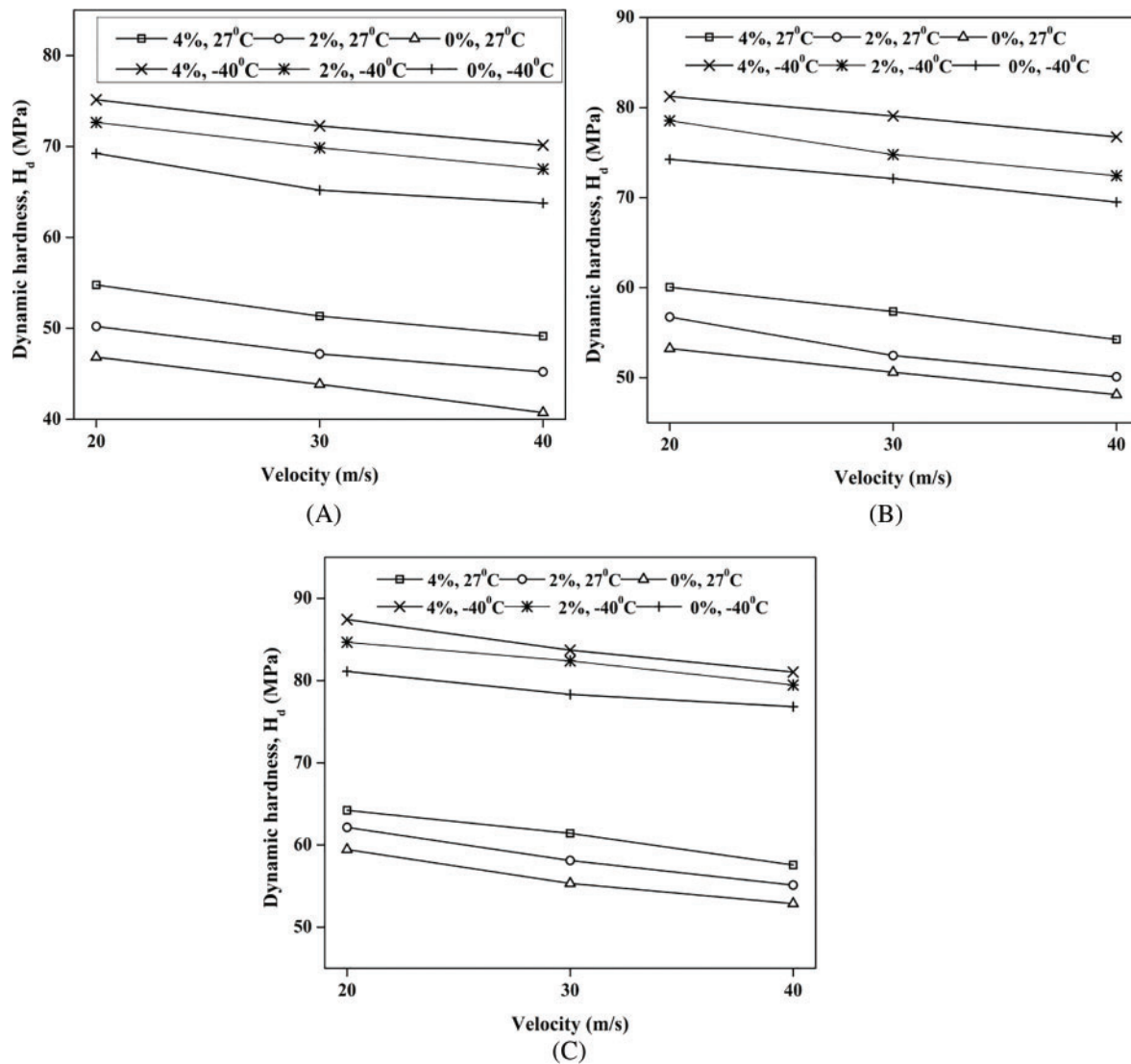


**Figure 6:** (A) Dynamic hardness of ZnO filled jute/epoxy; (B) Dynamic hardness of TiO<sub>2</sub> filled jute/epoxy; (C) Dynamic hardness of ZrO<sub>2</sub> filled jute/epoxy

### 3.3 Interfacial Properties of Filled Jute/Epoxy Composites

The Fig. 8A,B presented here is from the 4 wt.% filled ZrO<sub>2</sub> jute/epoxy composite tested at ambient temperature, sub-zero temperature conditions, and all other filler combinations and weight percentages of the filler follow similar failure mechanisms with varying extent of the damage. The figures show that the difference in the matrix behaviour and the jute fiber at sub-zero temperatures will result in matrix cracks. The fiber pull out and matrix cracks, are some of the common deformation and damage observed in jute/epoxy composite and any other continuous fiber composites tested under projectile impact loading as shown in Fig. 8A,B. The fiber break and the matrix deformation can lead to improved strength of the jute/epoxy composite at ambient temperature conditions. The brittle nature of the fiber, fiber delamination, and weak interface bonding generates fiber failures. The impact

resistance of the filled jute/epoxy composites are improved with the addition of nanofillers and the exposure of the hybrid composites to sub-zero temperatures as shown in Fig. 8B.

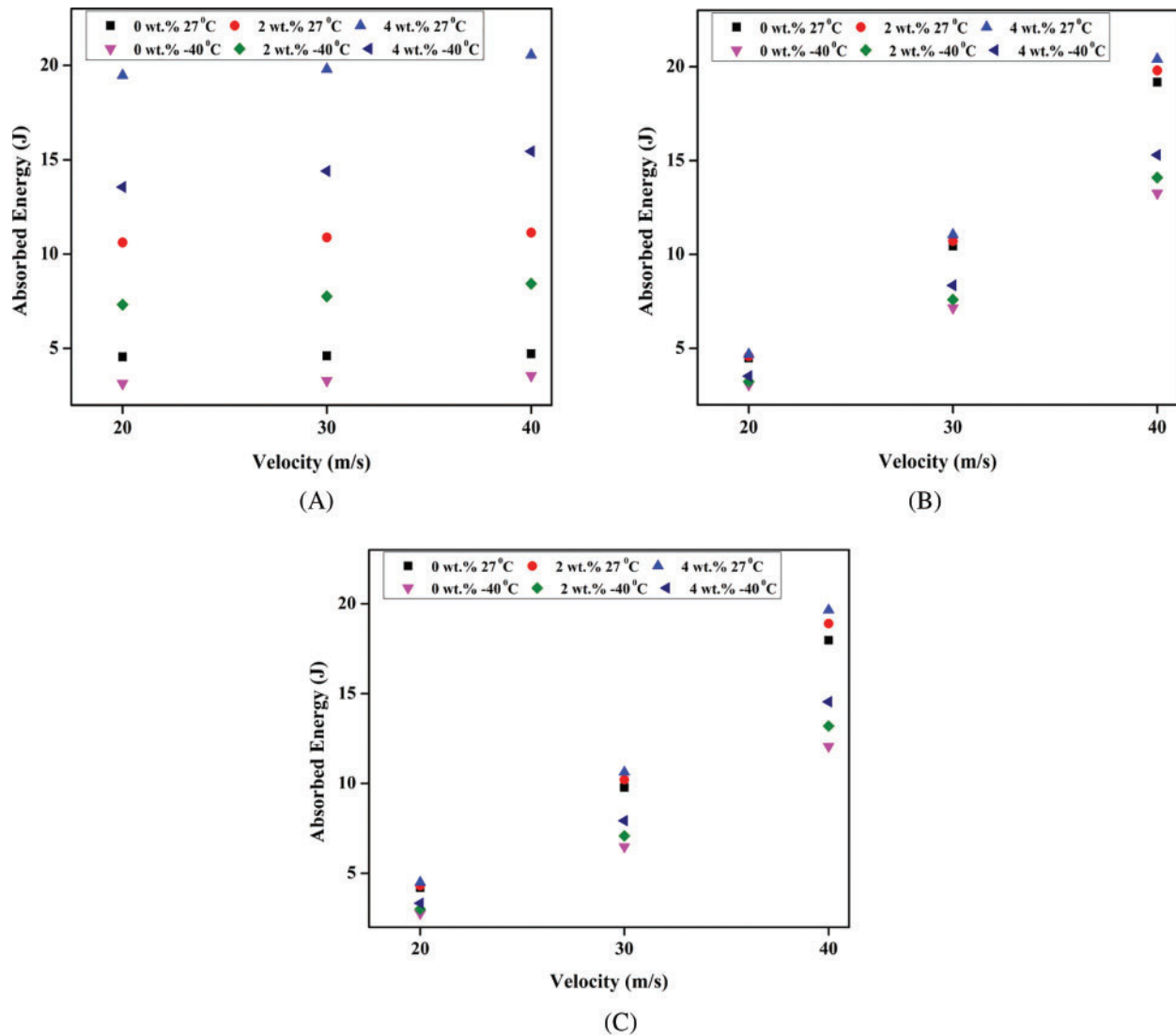


**Figure 7:** (A) Absorbed energy of ZnO filled jute epoxy composites; (B) Absorbed energy of TiO<sub>2</sub> filled jute epoxy composites; (C) Absorbed energy of ZrO<sub>2</sub> filled jute epoxy composites

### 3.4 Pre and Post-Impact Natural Frequency

The hybrid jute/epoxy composite plates clamped at the four sides are subjected to excitation using an impact hammer before impact and after the impact event to obtain the natural frequencies. The response of the excitation is obtained with an accelerometer pick-up and converted to FRF plots using the m + p Analyzer. The frequency resolution used for vibration analysis of filled jute/epoxy plates is 3.125 Hz and the signal time length is 0.32 s. The Fig. 9A–C shows the natural frequency for the first mode of vibration of laminates filled with various fillers in 2, 4 wt.% filler addition. The filled composites are subjected to different projectile velocities of 40, 30 and 20 m/s. The natural frequency is found to increase as the percentage of filler increases irrespective of the various fillers added to the laminates.

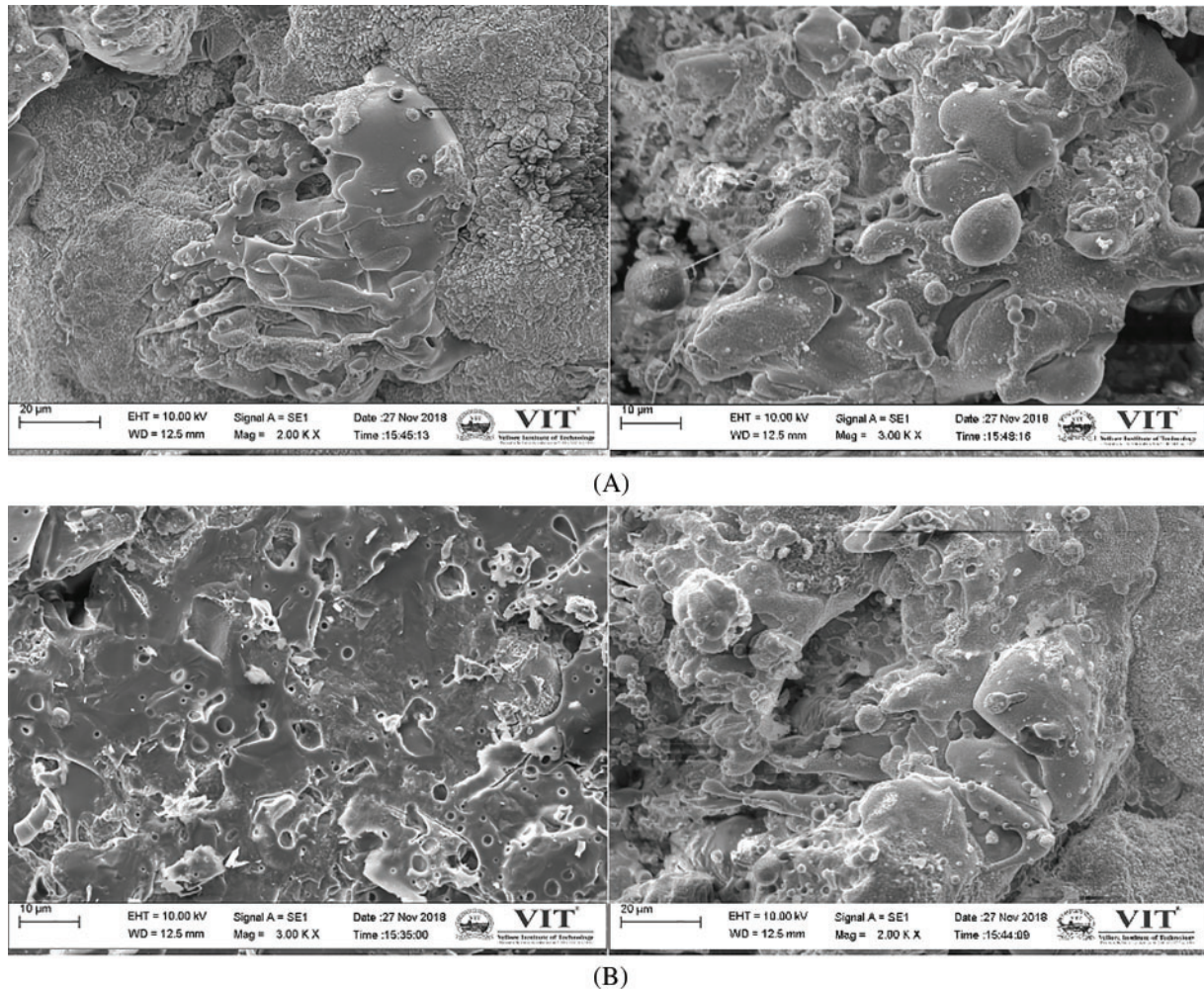


**Figure 8:** (A) Matrix crack initiation and fiber pull out of  $ZrO_2$  filled composites at ambient temperature; (B) Matrix crack initiation and fiber pull out of  $ZrO_2$  filled composites at subzero temperature

Free vibration behavior and dynamic mechanical analysis can effectively be used to find the complex modulus of the filled composites. The elastic behavior represents the complex modulus's real part and defines the stiffness of the composite. The addition of the nano-fillers increases both the stiffness and the modulus of the filled composites and hence the natural frequency also increases as the weight percentage of the filler increases. Irrespective of the fillers the natural frequency of the hybrid composites improved to a greater extent on filler addition up to 4% in weight. With increasing impact velocity, the change in natural frequency is higher and lower for the different modes of vibration of the unfilled composite plate and filled hybrid composite plates, respectively. The natural frequency increases with the inclusion of fillers, irrespective of the filler type for velocities of impact ranging from 20 to 40 m/s. The presence of nanofillers in the laminate restricts the delamination upon impact loading thereby improving the natural frequency of the filled composites as with the unfilled jute/epoxy composites. The anti-plasticization effect as a result of the polymer chain disruption improves the energy absorption and stiffness of the hybrid jute/epoxy composites at sub-zero temperatures. The hybrid composites experience only partial molecular chain reversibility after liquid nitrogen exposure.

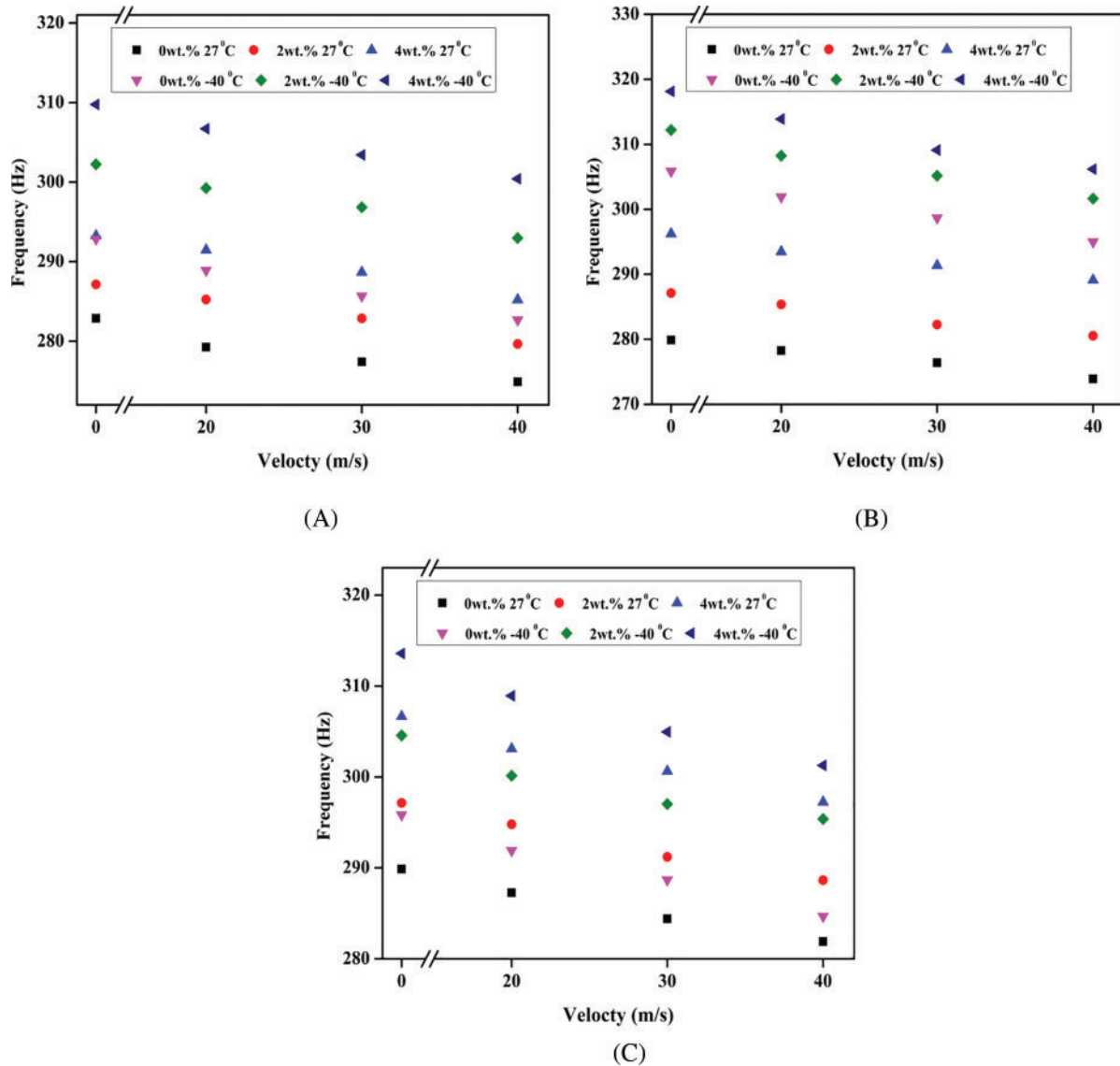


**Figure 9:** (A) Natural frequency of TiO<sub>2</sub> filled nanocomposites at different temperatures before and after impact; (B) Natural frequency of ZnO filled nano-composites at different temperatures before and after impact; (C) Natural frequency of ZrO<sub>2</sub> filled nano-composites at different temperatures before and after impact

The frequency increase up to 4 wt.% of filler addition and above 4 wt.% both parameters exhibit a decreasing trend due to the weak matrix-filler interface and agglomeration. The interfacial shear strength between the matrix and nanofiller in filled composites at sub-zero conditions is higher as there is the formation of thicker interphases and cross-linked polymer chains.

### 3.5 Pre and Post-Impact Loss Factor

The jute epoxy-filled hybrid composite material properties are dependent on frequency and temperature. The hybrid jute epoxy composite has low damping and higher storage modulus in the glassy state. As the temperature increases the filled jute epoxy composite exhibits several maxima as

the degree of damping is concerned with the change in modulus. The damping is maximum for a lower value of storage modulus for the jute epoxy composite. The stiffness and damping behavior of the hybrid composite are influenced by the frequency gains. Also, the maximum molecular mobility is observed at the temperature of maximum damping.

The damping of fiber composites can be related to the complex Young's modulus considering the composite's viscoelastic nature. The nanofillers improve the damping factor, natural frequency, and the improvement is noticed for filler addition up to 4% weight as shown in Fig. 10A–C. The rigid nanoparticle causes inelastic deformation of the epoxy matrix and creates micro-cracks due to higher stress concentration in the proximity of the fillers. The cross-link formation and thin interfaces between the matrix and fillers improve the interfacial shear strength in filled nanocomposites compared to the micro composites. The thermal conductivity and the movement of the polymer chains are proportional at lower temperatures. Here as the  $ZrO_2$  nanofillers have the lowest thermal conductivity (2 W/m·K), the movements of the chain are highly restricted in the  $ZrO_2$  filled jute/epoxy hybrid composites resulting in higher stiffness and higher damping factor compared to the other two filler combination.

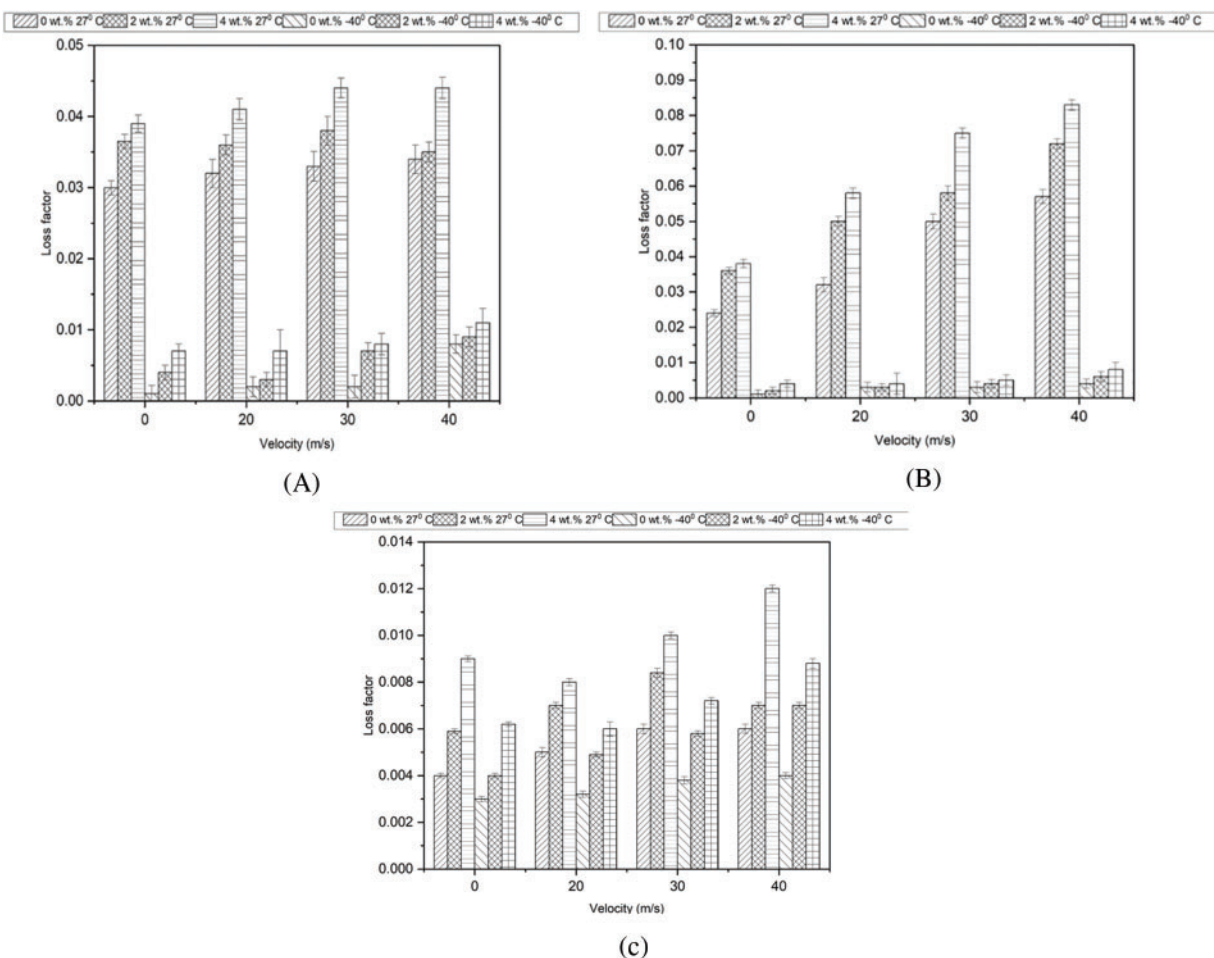


**Figure 10:** (A) Loss factor of ZnO filled jute/epoxy composites at different temperatures and velocities; (B) Loss factor of  $TiO_2$  filled jute/epoxy composites at different temperatures and velocities; (C) Loss factor of  $ZrO_2$  filled jute/epoxy composites at different temperatures and velocities

### 3.6 Damage Area

As the initial velocity of the impact event increases from 20 to 40 m/s the damage area increases and the natural frequency decreases. The change in natural frequency is higher in the laminates without filler addition which shows that the addition of filler limits the change in natural frequency. The delamination of the filled laminates is also less compared to the unfilled laminates for a corresponding velocity which also justifies the natural frequency change. In all the laminates the damage area is higher at the bottom face of the laminate compared to the top face due to the composite plate bending during impact and the distribution of the multi-axial impact forces. The damage area in the unfilled laminate is calculated to be 1915.68 mm<sup>2</sup> at 40 m/s and the damage area at 20 m/s is 488.27 mm<sup>2</sup>. The damaged area of the ZrO<sub>2</sub> filled hybrid laminates is minimum (1094.42 mm<sup>2</sup> at 40 m/s and 278.89 mm<sup>2</sup> at 20 m/s) while the laminates filled with ZnO show higher extent of the damage. The smaller particle size, interfacial interactions between filler and matrix, and higher density of ZrO<sub>2</sub> fillers lead to better stress transfer to the fillers in the filled composites. The restriction in the mobility of the polymer chains also contributes to the extent of damage in the filled composite. The increased surface area of the ZrO<sub>2</sub> nano fillers results in larger volumes of matrix filler interface and leads to enhanced stress transfer resulting in lower damage areas compared to the ZnO filled composites. Also, the damage area is minimal in 4% filled laminates and maximum in the 2% filled laminates irrespective of the filler used.

## 4 Conclusion

This research aims to assess the dynamic behavior of the jute/epoxy composites reinforced with ceramic fillers ZnO, TiO<sub>2</sub> and ZrO<sub>2</sub>. The dynamic behavior of the jute/epoxy nanocomposite shows that the natural frequency of the composite has an increasing trend as the nanofillers increase from 0% to 4%. The natural frequency also increases with sub-zero temperature conditions. As the impact velocity and temperature decrease, the coefficient of restitution increases. The addition of fillers in various weight percentages improves the damping and natural frequency of the hybrid laminates. The percentage decrease in natural frequency after ballistic impact is 3.06 and 3.92 at room temperature and sub-zero temperature respectively for ZrO<sub>2</sub> filled composites. The damping factor increases 33.33% and 25.75% for 4% ZrO<sub>2</sub> filled composites with the increase in velocity.

The damping factor increases as temperature increases and at the sub-zero temperature, the damping factor has comparatively lower values, 25% less compared to room temperature. The damping factor increases 11.05% at room temperature and 20.87% at sub-zero temperatures with an increase in filler addition for ZrO<sub>2</sub> filled composites.

The addition of ZrO<sub>2</sub> has limited the damaged area by 57.13% and 51.02% at room temperature and sub-zero temperature respectively compared to the unfilled condition. The filler that is found to be the best from the dynamic characteristics evaluated at ambient and sub-zero temperature testing is ZrO<sub>2</sub>.

**Acknowledgement:** The authors express their gratitude to Vellore Institute of Technology, Chennai for the support to carry out this work.

**Funding Statement:** The authors received no specific funding for this study.

**Author Contributions:** Somasundaram Karthiyaini: Research methodology, writing, and editing. Somasundaram Karthiyaini: Research methodology, writing, and editing. Abraham Jebamalar: Research methodology, writing, and editing. PA Prasob: Study conceptual, experimental implementation, and writing the original draft. All authors reviewed the results and approved the final version of the manuscript.



**Availability of Data and Materials:** Data availability exists in the form of tables, figures, and references.

**Ethics Approval:** Not applicable.

**Conflicts of Interest:** The authors declare no conflicts of interest to report regarding the present study.

## References

1. Wang A, Liu X, Yue Q, Xian G. Comparative study on the low-velocity impact properties of unidirectional flax and carbon fiber reinforced epoxy plates. *Mech Adv Mater Struct.* 2024;31(16):3531–42. doi:10.1080/15376494.2023.2179705.
2. Mishra T, Mandal P, Sahoo D. A state-of-the-art review on potential applications of natural fiber-reinforced polymer composite filled with inorganic nanoparticle. *Composit Part C: Open Access.* 2022;9:100298. doi:10.1016/j.jcomc.2022.100298.
3. Shah S, Karuppanan S, Megat-Yusoff P, Sajid Z. Impact resistance and damage tolerance of fiber reinforced composites: a review. *Compos Struct.* 2019;217:100–21. doi:10.1016/j.compstruct.2019.03.021.
4. Gull N, Khan SM, Munawar MA, Shafiq M, Anjum F, Butt MTZ, et al. Synthesis and characterization of zinc oxide (ZnO) filled glass fiber reinforced polyester composites. *Mater Design.* 2015;67:313–7. doi:10.1016/j.matdes.2014.11.021.
5. Zhang D, Zhang X, Luo Y, Wang Q. Experimental study on drop-weight impact response of basalt fiber aluminum laminates (BFMLs). *Adv Mater Sci Eng.* 2018;2018(1):1478951. doi:10.1155/2018/1478951.
6. Mohan S, Velu S. Ballistic impact behaviour of unidirectional fibre reinforced composites. *Int J Imp Eng.* 2014;63:164–76. doi:10.1016/j.ijimpeng.2013.07.008.
7. Prasob PA, Sasikumar M, Tamil Selvan P. Impact behaviour of PMC reinforced with fibers under subzero temperature: a review. *Indian J Sci Tec.* 2016;33:1–10. doi:10.17485/ijst/2016/v9i33/88737.
8. Pandya KS, Kumar CVS, Nair NS, Patil PS, Naik NK. Analytical and experimental studies on ballistic impact behavior of 2D woven fabric composites. *Int J Dam Mec.* 2015;24(4):471–511. doi:10.1177/1056789514531440.
9. Ma H-L, Jia Z, Lau K-T, Leng J, Hui D. Impact properties of glass fiber/epoxy composites at cryogenic environment. *Comp Part B: Eng.* 2016;92(7):210–17. doi:10.1016/j.compositesb.2016.02.013.
10. Dimeski D, Srebrenkoska V, Mirceska N. Ballistic impact resistance mechanism of woven fabrics and their composites. *Int J Eng Res Tec.* 2015;4(12):107–12.
11. Sikarwar RS, Velmurugan R. Ballistic impact on glass/epoxy composite laminates. *Def Sci J.* 2014;64(4):393–99. doi:10.14429/dsj.64.3882.
12. Reddy PRS, Reddy TS, Madhu V, Gogia AK, Rao KV. Behavior of E-glass composite laminates under ballistic impact. *Mater Des.* 2015;84:79–86. doi:10.1016/j.matdes.2015.06.094.
13. Shen Z. Characterisation of low velocity impact response in composite laminates (Doctoral Dissertation). School of Engineering and Technology, University of Hertfordshire: UK; 2015. doi:10.18745/th.16334.
14. Zhang D, Sun Y, Chen L, Pan N. A comparative study on low-velocity impact response of fabric composite laminates. *Mater Des.* 2013;50:750–6. doi:10.1016/j.matdes.2013.03.044.
15. Andrew J, Jefferson. Parameters influencing the impact response of fiber-reinforced polymer matrix composite materials: a critical review. *Comp Stru.* 2019;224:111007. doi:10.1016/j.compstruct.2019.111007.
16. Kang TJ, Kim C. Energy-absorption mechanisms in kevlar multiaxial warp-knit fabric composites under impact loading. *Comp Sci Tec.* 2000;60(5):773–84. doi:10.1016/S0266-3538(99)00185-2.
17. Balaganesan G, Velmurugan R, Srinivasan M, Gupta NK, Kanny K. Energy absorption and ballistic limit of nanocomposite laminates subjected to impact loading. *Int J Imp Eng.* 2014;74:57–66. doi:10.1016/j.ijimpeng.2014.02.017.
18. Kumar CS, Arumugam V, Dhakal HN, John R. Effect of temperature and hybridisation on the low velocity impact behavior of hemp-basalt/epoxy composites. *Comp Stru.* 2015;125(3):407–16. doi:10.1016/j.compstruct.2015.01.037.
19. Mathivanan NR, Jerald J. Experimental investigation of woven E-glass epoxy composite laminates subjected to low-velocity impact at different energy levels. *J Min Mater Char Eng.* 2010;9(7):643–52. doi:10.4236/jmmce.2010.97046.

20. Omar N, Mohd S, Najwa S, Aminanda Y, Syed Mohamed Ali J, Kashif SM. Experimental observation of jute/epoxy composite plate subjected to impact loading. *ICMAAE*. 2011;11:1–5.
21. Kulkarni SM, Sunil D, Sharathchandra S. Effect of surface treatment on the impact behaviour of fly-ash filled polymer composites. *Poly Int*. 2002;51(12):1378–84. doi:10.1002/pi.1055.
22. Navaranjan N, Neitzert T. Impact strength of natural fibre composites measured by different test methods: A review. *MATEC Web Conf*. 2017;109:01003. doi:10.1051/mateconf/201710901003.
23. Sikarwar RS, Velmurugan R, Gupta NK. Influence of fiber orientation and thickness on the response of glass/epoxy composites subjected to impact loading. *Comp Part B: Eng*. 2014;60:627–36. doi:10.1016/j.compositesb.2013.12.023.
24. Liu H, Liu J, Kaboglu C, Zhou J, Kong X, Blackman BR, et al. The behaviour of fibre-reinforced composites subjected to a soft impact-loading: an experimental and numerical study. *Eng Fail Anal*. 2020;111:104448. doi:10.1016/j.engfailanal.2020.104448.
25. García-Castillo SK, Sánchez-Sáez S, López-Puente J, Barbero E, Navarro C. Impact behaviour of composite panels subjected to in-plane load. In: 16th International Conference on Composite Materials, 2007; Kyoto, Japan.
26. Prakash NB, Madhusudhan T. Investigative study on impact strength variation in different combination of polymer composites. *Int J Eng Res Gen Sci*. 2015;3:2091–110.
27. Naik NK, Sekher YC, Meduri S. Damage in woven-fabric composites subjected to low-velocity impact. *Comp Sci Tec*. 2000;60(5):731–44. doi:10.1016/s0266-3538(99)00183-9.
28. Gómez-del Río T, Zaera R, Barbero E, Navarro C. Damage in CFRPs due to low velocity impact at low temperature. *Comp Part B: Eng*. 2005;36(1):41–50. doi:10.1016/j.compositesb.2004.04.003.
29. Morye SS, Hine PJ, Duckett RA, Carr DJ, Ward IM. Modelling of the energy absorption by polymer composites upon ballistic impact. *Comp Sci Tec*. 2000;60(14):2631–42. doi:10.1016/s0266-3538(00)00139-1.
30. Wang X, Hu B, Feng Y, Liang F, Mo F, Xiong J, et al. Low velocity impact properties of 3D woven basalt/aramid hybrid composites. *Comp Sci Tec*. 2008;68(2):444–50. doi:10.1016/j.compscitech.2007.06.016.
31. Potti SV, Sun CT. Prediction of impact induced penetration and delamination in thick composite laminates. *Inter J Imp Eng*. 1997;19(1):31–48. doi:10.1016/s0734-743x(96)00005-x.
32. Ahmadi M, Ansari R, Hassanzadeh-Aghdam MK. Low velocity impact analysis of beams made of short carbon fiber/carbon nanotube-polymer composite: a hierarchical finite element approach. *Mec Adv Mater Stru*. 2019;26(13):1104–14. doi:10.1080/15376494.2018.1430276.
33. Oskouie MF, Hassanzadeh-Aghdam MK, Ansari R. A new numerical approach for low velocity impact response of multiscale-reinforced nanocomposite plates. *Eng Comp*. 2021;37:713–30. doi:10.1007/s00366-019-00851-9.
34. Rasoolpoor M, Ansari R, Hassanzadeh-Aghdam MK. Dynamic behavior of particulate metal matrix nanocomposite plates under low velocity impact. *Proc Inst Mec Eng Part C: J Mec Eng Sci*. 2020;234(1):180–95. doi:10.1177/0954406219875781.
35. Roy M. Dynamics of impact of sphere on flat surfaces of polymer matrix composites. *Bul Mater Sci*. 1999;22(6):1009–12. doi:10.1007/bf02745695.
36. Tatar AC, Kaybal HB, Ulus H, Demir O, Avcı A. Evaluation of low-velocity impact behavior of epoxy nanocomposite laminates modified with SiO<sub>2</sub> nanoparticles at cryogenic temperatures. *Res Eng Stru Mater*. 2019;5(2):115–25. doi:10.17515/resm2018.55is0704.
37. Kaybal HB, Ulus H, Demir O, Şahin ÖS, Avcı A. Effects of alumina nanoparticles on dynamic impact responses of carbon fiber reinforced epoxy matrix nanocomposites. *Eng Sci Tech Int J*. 2018;21(3):399–407.
38. Kaybal HB, Ulus H, Eskizeybek V, Avcı A. An experimental study on low velocity impact performance of bolted composite joints part I: influence of halloysite nanotubes on dynamic loading response. *Comp Stru*. 2021;258:113415. doi:10.1016/j.compstruct.2020.113415.

39. Kaybal HB, Ulus H, Eskizeybek V, Avcı A. An experimental study on low velocity impact performance of bolted composite joints–part 2: influence of long-term seawater aging. *Comp Stru.* 2021;272:113571. doi:10.1016/j.compstruct.2021.113571.
40. Eskizeybek V, Ulus H, Kaybal HB, Şahin ÖS, Avcı A. Static and dynamic mechanical responses of CaCO<sub>3</sub> nanoparticle modified epoxy/carbon fiber nanocomposites. *Comp Part B: Eng.* 2018;140:223–31. doi:10.1016/j.compositesb.2017.12.013.